Sawtooth control by on-axis electron cyclotron current drive on the WT-3 tokamak

M. Asakawa, K. Tanabe, , A. Nakayama*, M. Watanabe*,
M. Nakamura**, H. Tanaka*, T. Maekawa*, Y. Terumichi
Department of Physics,
Faculty of Science,
Kyoto University,
Kyoto 606-8502, Japan

Abstract

The experiments on control of sawtooth oscillations (STO) by electron cyclotron current drive (ECCD) have been performed on the WT-3 tokamak. Stabilization and excitation of STO are observed for counter-ECCD and co-ECCD, respectively, when the position of the power deposition is located inside the inversion radius. These results are due to the modification of the current profile near the magnetic axis.

1. INTRODUCTION

ECCD is a possible method for controlling the plasma current profile: it has the capability to focus and aim the EC wave power at any internal location in plasma in order to efficiently deposit the power locally. Especially, on-axis ECCD is effective to control the profile of safety factor near the magnetic axis , because the cross section of the power deposition is minimized, thus the current density of the driven-current is maximized. On the WT-3 tokamak (R_0=65cm, a=20cm, B_{t0} (MAX)=1.75 T), the experiments on control of STO by on-axis ECCD are carried out. In Ohmic heating plasma with a safety factor at the limiter, q_a=4.8, typical inversion radius of STO is 3cm. Assuming a current profile, the safety factor at the magnetic axis, q(0), is estimated to be 0.8 in this case. If a driven-current of 5kA anti-parallel to the plasma current, which is only 5% of the total plasma current, is generated inside the inversion radius, q(0) rises to 1.2 and the q(r)=1 surface disappears.

In order to concentrate the EC wave power near the magnetic axis, the gyrotron output (frequency = 89GHz, max. power =150kW) is focused near the center of torus using a quasi-optical transmission system [1]. The elliptical Gaussian power distribution measured with a thermal image camera has radii of 0.8cm in the direction parallel to the major axis and 1.3cm in the toroidal direction at the focal point. By tilting the launching mirror, the launch angle is varied, and the index of refraction parallel to the magnetic field $N_{//}$ is changed from -0.6 to 0.6. Also the launch angle to the equatorial plane can be varied. The EC wave is obliquely launched from the low-magnetic field side in the extraordinary mode. The evolution of STO is investigated by using soft X ray (SX) computerized tomograph (CT) which consists of 100 SX detectors.[2]

2. STO CONTROL BY ON-AXIS ECCD

The EC waves are injected into Ohmic heating discharges with the plasma current I_p=100 kA and line average electron density n_e=0.5 $\sim 10^{13}$cm^{-3}, in which STO are steadily excited. The position $R_{2\Omega ce}$, where $\omega=2\Omega_{ce}$ is satisfied, is fixed near the center of torus during the experiments. Fig. 1 shows the typical plasma response to the EC wave injection in the cases of $N_{//}$=0.56 and $N_{//}$=-0.56. Here, co- and counter-injection indicate the EC wave injection with $N_{//}$>0 and $N_{//}$<0,

*Present address: Department of Fundamental Energy Science, Graduate School of Energy Science, Kyoto University, Kyoto 606-8502, Japan

**Present address: Osaka Institute of Technology, Osaka 535, Japan

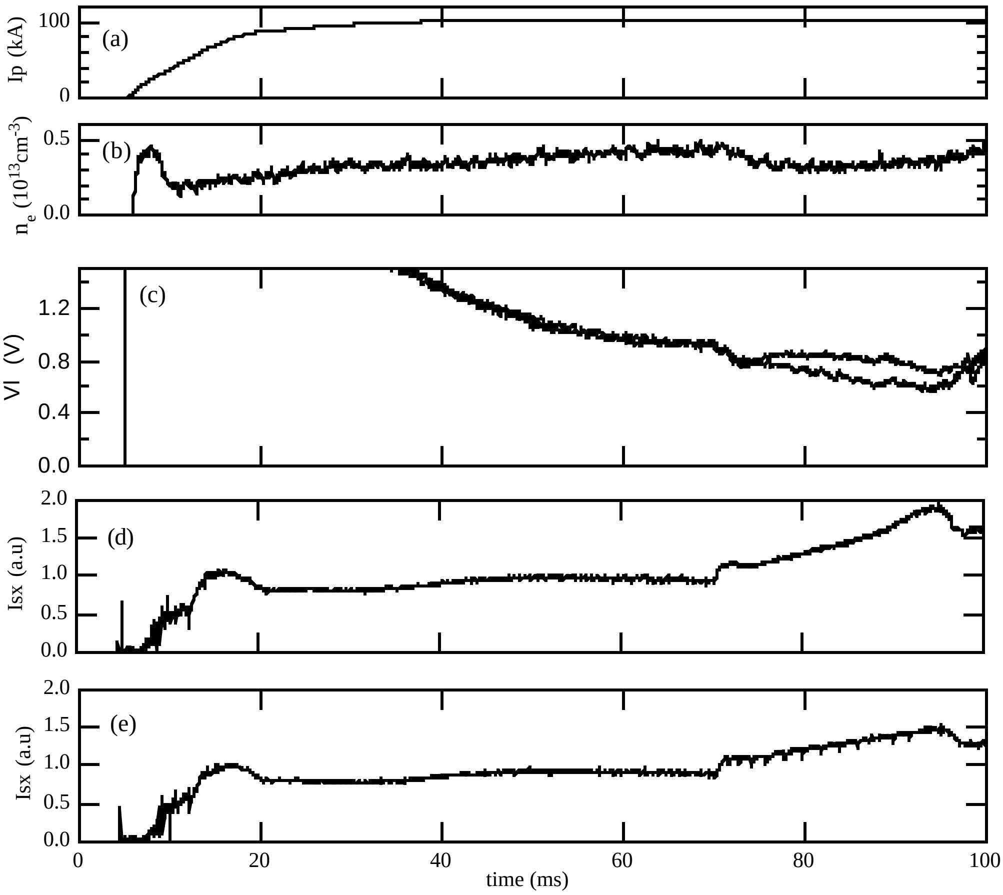

Fig.1 Time traces of (a) plasma current I_p, (b) line average density n_e, (c) loop voltages, and soft-X ray signals, I_{sx}, for (d) co-injection ($N_{//}$=0.56) and (e) counter-injection ($N_{//}$=-0.56). EC wave of 140 kW is injected during 70ms to 95ms.

respectively. The EC wave propagates in the direction of electron drift for co-injection, while the EC wave propagates in the direction of I_p for counter-injection. There are no notable differences in I_p (Fig.1(a)) and n_e (Fig1(b)) between co- and counter-injection, but there are differences in the loop voltage and STO observed in the soft X-ray signals. 1) The loop voltage for counter-injection is higher than that for co-injection (Fig.1(c)). 2) STO are enhanced for co-injection (Fig.1 (d)), while they are stabilized for counter-injection (Fig.1(e)). The loop voltage falls from its value for the perpendicular injection ($N_{//}$=0) with increasing $N_{//}$ for co-injections, and increases with increasing $|N_{//}|$ for counter-injections. It is inferred that the differences of the loop voltages for different $N_{//}$ are attributed to the driven current by ECCD. Assuming that the resistivity is identical for the discharges with the same $|N_{//}|$ and that the amount of the driven current I_{eccd} does not depend on the directions of ECCD, I_{eccd} is derived from the comparison between the loop voltages for co- and counter-injection:

$$I_{eccd}=\frac{V_{cntr}-V_{co}}{V_{cntr}+V_{co}}I_p \, .$$

In the range of $|N_{//}|<0.4$, I_{eccd} increases with increasing $|N_{//}|$ and remains almost constant in the range of $0.4<|N_{//}|<0.6$ as shown in Fig.2. In the cases of counter-injections, in which the driven current is anti-parallel to I_p, the periods of STO become longer as $|N_{//}|$ increases up to 0.4, then the STO are stabilized for discharges with $|N_{//}|>0.4$ and I_{eccd} > 6kA. In contrast, STO increase their amplitudes during co-injection, in which the driven current is parallel to I_p. In this case, their periods are shorter than those of perpendicular injection.

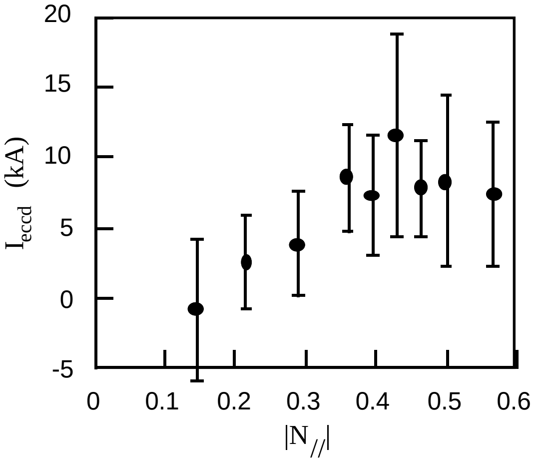

Fig.2 Dependence of driven current I_{eccd} on $|N_{//}|$.

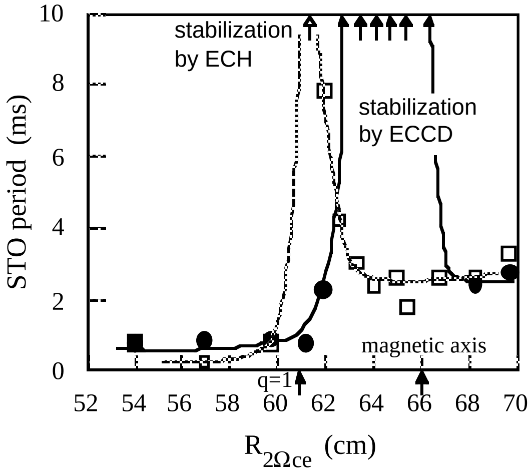

Fig.3 Dependence of sawtooth period on $R_{2\Omega ce}$. Solid circles indicate in the case of counter-ECCD, and solid squares indicate in the case of ECH

The driven current I_{eccd} at $|N_{//}|$=0.56 and the response of STO are investigated as a function of $R_{2\Omega ce}$ by changing the toroidal field shot by shot. The maximum of I_{eccd} is observed at $R_{2\Omega ce}$ =64cm, and I_{eccd} is significant in the range of 62cm<$R_{2\Omega ce}$ <67cm. During these experiments, the position of magnetic axis estimated using magnetic probes is R=66cm. Thus the maximum I_{eccd} is observed when $R_{2\Omega ce}$ is displaced by 2cm from the magnetic axis toward the high-field side. As shown in Fig.3, STO are stabilized by ECH at $R_{2\Omega ce}$=61cm, corresponding to the position of the inversion radius estimated by SXCT, while the stabilization takes place when $R_{2\Omega ce}$ is located inside the inversion radius for counter-ECCD.

The driven current I_{eccd} and the response of STO are also investigated as a function of the injection angle to the equatorial plane as shown in Fig.4(a). In these experiments, the toroidal field is set to be as $R_{2\Omega ce}$ =64cm. Maximum of I_{eccd} is observed when the beam axis of EC wave passes through the magnetic axis, and I_{eccd} decreases as the beam axis moves farther from the magnetic axis. As shown in Fig.4(b), STO is stabilized by ECH when the beam axis is aimed to the intersections of EC resonant layer and the inversion radius, while stabilization of STO is observed for counter-ECCD when the beam axis passes inside the inversion radius. Because the beam radius is smaller than the inversion radius, this result suggests that the stabilization by counter-ECCD is associated with the power deposition inside the inversion radius. Thus, it is inferred that the stabilization is caused by the decrease of the current inside the inversion radius.

Also the result shown in Fig.3 suggests the STO stabilization for counter-ECCD is due to the decrease of the current density near the magnetic axis, because only the electrons moving parallel to I_p can be selectively heated by counter-ECCD around the magnetic axis when $R_{2\Omega ce}$ is shifted toward the high-field side from the magnetic axis. Thus the current density near the magnetic axis decreases. As a result, the safety factor at the magnetic axis q(0) is inferred to rise higher than unity.

ECCD experiments are also performed in Ohmic heating discharges with I_p=70kA and n_e=0.5 ~$10^{13}cm^{-3}$, in which STO are not excited. In this case, STO are excited by co-ECCD. The excitation of STO by co-ECCD is inferred due to the increase of the current density near the magnetic axis which leads q(0) to fall below unity.

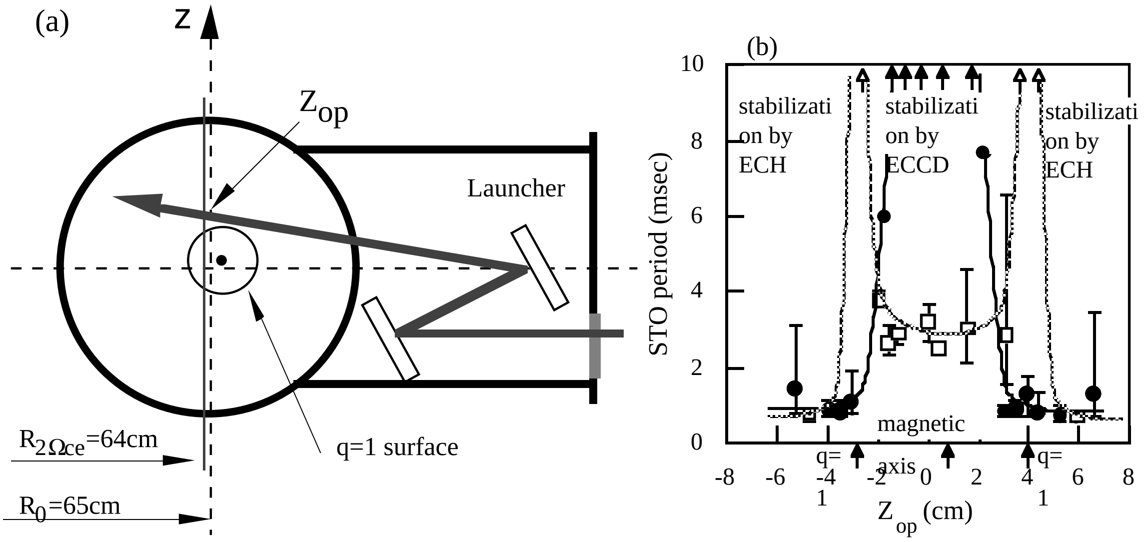

Fig.4 (a) The injection angle to the equatorial plane is changed by tilting the launcher. In the case of counter-ECCD, $N_{//}$=-0.56. Z_{op} denotes the intersection of the beam axis of EC wave and Z-axis, which is parallel to the major axis of the torus. (b) Dependence of the STO period on Z_{op}. Solid circles indicate in the case of counter-ECCD, and open squares indicate in the case of ECH

3. SUMMARY

The experiments on STO control by on-axis ECCD are performed on WT-3. While STO are stabilized by ECH on the inversion radius, the stabilization is observed for the counter-ECCD with following conditions;
(1) discharges with $|N_{//}|$>0.4, in which the I_{eccd} exceeds 6kA,
(2) $R_{2\Omega ce}$ is located inside the inversion radius,
(3) the EC wave passes through inside the inversion radius.
These results suggest that the stabilization is due to the decease in the current density near the magnetic axis caused by the counter-ECCD. It is inferred that the decrease in current density rises q(0) higher than unity, and then q=1 surface disappears from the plasma.

In contrast to the counter-ECCD, STO are excited by the on-axis co-ECCD. The excitation is inferred due to the increase in the current density near the magnetic axis.

Acknowledgement

This work was supported by a Grant-in Aid for Scientific Research from the Ministry of Education in Japan.

REFERENCES

[1] Proceedings of the 1996 International Conference on Plasma Physics, vol.1, 9I01 (1996) 1010.

[2] Y. Terumichi et al., in Plasma Phys. and Contr. Nucl. Fusion Research 1990 (Proc. 13th Int. Conf. Washington), vol.1, IAEA, Vienna (1991) 777.